MEASURING TEMPORAL PHOTON BUNCHING IN BLACKBODY RADIATION

P. K. TAN[1,2], G. H. YEO[2], H. S. POH[1], A. H. CHAN[2], AND C. KURTSIEFER[1,2]
[1] Center for Quantum Technologies, 3 Science Drive 2, 117543, Singapore; pengkian@physics.org, phyck@nus.edu.sg
[2] Department of Physics, National University of Singapore, 2 Science Drive 3, 117551, Singapore

ABSTRACT

Light from thermal blackbody radiators such as stars exhibits photon bunching behavior at sufficiently short timescales. However, with available detector bandwidths, this bunching signal is difficult to observe directly. We present an experimental technique to increase the photon bunching signal in blackbody radiation via spectral filtering of the light source. Our measurements reveal strong temporal photon bunching from blackbody radiation, including the Sun. This technique allows for an absolute measurement of the photon bunching signature $g^{(2)}(0)$, and thereby a direct statement on the statistical nature of a light source. Such filtering techniques may help revive the interest in intensity interferometry as a tool in astronomy.

Key words: instrumentation: interferometers – radiation mechanisms: thermal – stars: fundamental parameters – Sun: fundamental parameters – techniques: interferometric

Online-only material: color figures

1. BACKGROUND

Statistical intensity fluctuations from stationary thermal light sources formed the basis of the landmark experiments by Hanbury-Brown & Twiss (1954, 1957), where correlation measurements between a pair of photodetection signals were used to assess both temporal and spatial coherence properties of light fields. The explanation for these fluctuations as photon bunching phenomena, as compared to a Poissonian distribution for uncorrelated detection processes, was a major contribution for the development of the field of quantum optics (Glauber 1963).

Hanbury-Brown & Twiss (1956) and Hanbury-Brown et al. (1974) developed their observation into a spatial intensity interferometer that allowed them to infer stellar angular radii from the spatial coherence properties of starlight over relatively large distances of 188 m. Since a key quality of any telescope system is its angular resolution, given by its real or virtual aperture, they managed to carry out these measurements with unprecedented accuracy. Yet, the comparatively simple optical intensity interferometry technique has not found widespread adoption in the observation of celestial objects due to a relatively small signal-to-noise ratio (S/N) in measuring the spatial decay of the photon bunching signature (Davis et al. 1999; Millour 2008).

Typically, the photon bunching signature is observed in a regime where the ratio of the coherence time, τ_c, over the photodetector resolution, τ_t, is significantly smaller than one, even after an increase of the coherence time via optical filtering. In such a regime, the temporal coherence properties cannot be resolved directly, and the S/N in observing photon bunching is independent of the filter bandwidth (Hanbury-Brown 1974; Foellmi 2009; Rou et al. 2012; Nuñez 2012; Malvimat et al. 2013).

However, the temporal coherence properties may contain interesting information about the celestial light source, and help, e.g., to assess the spectra of Wolf–Rayet stars (Castor & Nussbaumer 1972; Varshni & Nasser 1986; van der Hucht 2001), such as Eta Carinae, with suspected laser emission lines estimated to be ≈50 MHz or less (Dravins & Germanà 2008), which are too narrow to resolve by conventional spectroscopy.

To understand the nature of the light of these very narrow spectral features, the suppression of a wide blackbody radiation background would be helpful.

Furthermore, in the regime of $\tau_c/\tau_t > 1$, one is also able to resolve the thermal character explicitly and to test for the thermal photon bunching signature of $g^{(2)}(0) = 2$. This permits the distinction between thermal and laser emission mechanisms for the discrete spectral components of Wolf–Rayet stars.

2. THE PROBLEM

Temporal photon bunching, i.e., the tendency for photons to cluster together on a short timescale, has been consistently observed from narrowband quasi-thermal light sources such as low-pressure glow discharge lamps (Martienssen & Spiller 1964; Morgan & Mandel 1966), and laser beams (Asakura 1970) that are passed through a rotating ground glass to randomize the optical phase in time.

Photon bunching in time for stationary fields is quantified by a second-order correlation function $g^{(2)}(\tau)$, which is the probability of observing a second photodetection event at a time τ after a first one, normalized to the probability of an uncorrelated detection. Optical modes in thermal states are the textbook example where $g^{(2)} = 2$ (Glauber 1963; Mandel & Wolf 1995; Saleh & Teich 2007). Blackbody radiation would therefore be the obvious choice for observing photon bunching, if it were not for the short coherence time associated with its spectral properties.

In a scenario where spatial coherence effects are neglected, the second-order temporal correlation function for light fields can be written as

$$g^{(2)}(\tau) = 1 + |\gamma(\tau)|^2 , \qquad (1)$$

where $\gamma(\tau)$ is the complex degree of coherence, or normalized self-coherence of the stationary light field with $\gamma(0) = 1$, which itself is proportional to the Fourier transform of the spectral density $S(\nu)$ of the light field (Mandel & Wolf 1995). For well-defined spectral densities and coherence functions, a meaningful coherence time τ_c can be defined, which is reciprocal to a characteristic width $\Delta\nu$ of the spectral distribution $S(\nu)$.
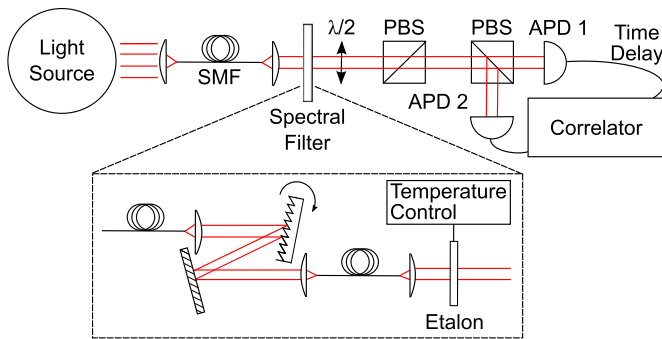
Figure 1. Setup to determine the temporal correlation $g^{(2)}(\tau)$ for wide-band thermal light. The initial spectrum gets filtered to a narrow optical bandwidth such that the temporal decay of the second-order correlation function can be observed with conventional single-photon detectors in a Hanbury-Brown–Twiss experiment. We employ a combination of a grating and a temperature-tuned etalon as a spectral filter, and ensure spatial coherence in the setup by using single-mode optical fibers (SMF).

(A color version of this figure is available in the online journal.)

For blackbody light sources in the optical regime, the coherence time τ_c given by Planck's law is on the order of 10^{-14} s, which is much shorter than the best timing resolution τ_t of a few 10^{-11} s for existing photodetectors. As shown by Scarl (1968), the observable excess from uncorrelated pair detections, $g^{(2)}(\tau = 0) - 1$, scales as τ_c/τ_t, and is thus only significant when the coherence time of the source is of the order of the detection timing response.

Therefore, empirical observation of temporal photon bunching from blackbody light sources has been extremely difficult, with only recent breakthroughs using two-photon absorption in semiconductors (Boitier et al. 2009) and in ghost imaging research using a narrowband Faraday anomalous dispersion optical filter (Karmakar et al. 2012; Liu et al. 2014).

In this Letter, we present a spectral filtering technique that significantly increases the observed temporal photon bunching signature from a blackbody light source.

3. EXPERIMENT

As with previous attempts to observe photon bunching from blackbody radiation (Karmakar et al. 2012; Liu et al. 2014), we employ narrowband optical filtering of the light source in order to increase the coherence time τ_c and use single-photon detectors with low timing uncertainties. The experimental setup is shown in Figure 1.

First, light from different sources under investigation is coupled into a single-mode optical fiber to enforce spatial coherence because the photon bunching signature $g^{(2)}(\tau = 0) - 1 \propto 1/M$, where M is the number of transverse modes (Glauber 1963).

The light is then collimated with an aspheric lens and sent through the first spectral filter, which is either an interferometric bandpass filter with an FWHM of 3 nm centered at 546.1 nm to match the $6p7s\,^3S_1$–$6p6s\,^3P_2^0$ transition in a mercury (Hg) discharge lamp, or a grating monochromator for the broadband continuous spectrum. While the interference filter is sufficient to select the spectral lines of the different mercury isotopes, the grating monochromator had to be used for the blackbody sources.

The core of the monochromator is a blazed reflective diffraction grating with 1200 lines mm^{-1} mounted on a rotation stage. Light from the optical fiber with a numerical aperture NA =
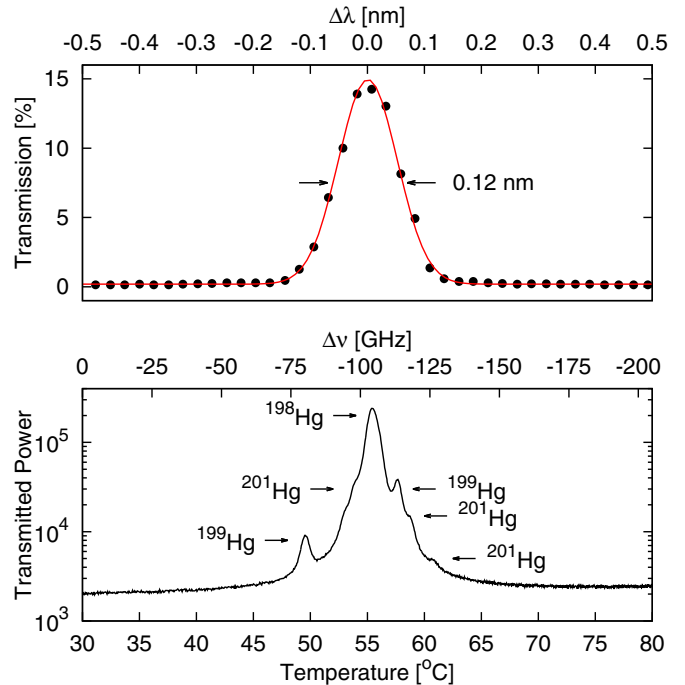

Figure 2. Top: transmission profile of grating monochromator. The solid line is a fit to a Gaussian profile to measurements for different grating angles (symbols), resulting in an FWHM of 0.122 ± 0.002 nm. Bottom: transmission of Hg light near 546 nm through the temperature-tuned etalon with 2 GHz bandwidth. The hyperfine structure for different isotopes is partially resolved, as identified in Sansonetti & Veza (2010).

(A color version of this figure is available in the online journal.)

0.13 is collimated with an achromatic doublet ($f = 30$ mm), illuminating about 10^4 lines of the grating. The first diffraction order is imaged with another achromat of ($f = 30$ mm) into another single-mode optical fiber. This arrangement acts as a tunable narrowband filter in the visible regime, allowing adjustment for peak emissions of blackbody light sources. A test of the transmission of a narrowband laser source ($\lambda = 532$ nm) is shown in Figure 2 (top part). The fit to a Gaussian transmission profile leads to an optical bandwidth of 0.122 ± 0.002 nm (FWHM). We typically observe a transmission of narrowband light from single-mode fiber to single-mode fiber of $\approx 15\%$.

In a second step, the light passed through a solid etalon (thickness $d = 0.5$ mm) with flat surfaces. The etalon has a free spectral range of FSR $= c/(2nd) = 205$ GHz, with a refractive index $n = 1.46$ for fused silica (Suprasil311), and the speed of light c in vacuum. At $\lambda = 546$ nm, the free spectral range corresponds to $\Delta\lambda = \lambda^2/c \cdot$ FSR ≈ 0.2 nm so that only one transmission order should fall within the monochromator transmission width. Both surfaces of the etalon have dielectric coatings with a reflectivity of $R \approx 97\%$ over a wavelength range from 390 nm to 810 nm, resulting in a transmission bandwidth (FWHM; Fox 2006) of

$$\Delta\nu \approx \text{FSR} \cdot \frac{1 - R}{\pi\sqrt{R}} \approx 2\,\text{GHz}. \qquad (2)$$

The central etalon transmission frequency is tuned by temperature, with a scaling of -4.1 GHz K^{-1} due to thermal expansion and temperature dependence of the refractive index. A temperature stability of ± 5 mK over the measurement duration of several hours ensures that the etalon stays on a specific wavelength. Temperature tuning allows the etalon to be always
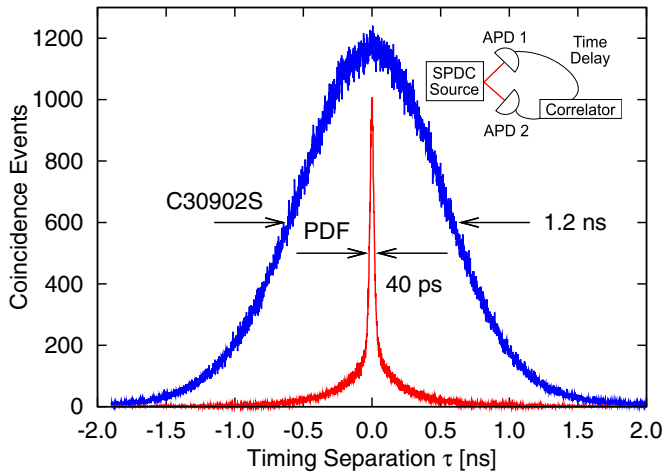
Figure 3. Comparison of timing jitter between two actively quenched thin avalanche photodiodes (PDF) and two passively quenched deep avalanche photodiodes (C90302S) by photon pair detection from light generated by spontaneous parametric down conversion (SPDC) with a coherence time below 10 ps.

(A color version of this figure is available in the online journal.)

used under normal incidence, which avoids frequency walk-off (Green 1980) and spatial distortion (Park et al. 2005). To demonstrate the resolving power of this device, we tuned the peak transmission across the various spectral lines from a Hg gas discharge lamp at 546.1 nm, revealing a partially resolved hyperfine structure for different isotopes (see Figure 2, bottom part).

A Glan–Taylor polarizer (PBS) following the etalon selects a well-defined linear polarization mode, with the same rationale of minimizing the number of modes that end up in the temporal correlation setup. A half-wave plate ($\lambda/2$) transforms the polarization emerging from the grating/fiber combination such that there is maximal transmission through the PBS.

A second Glan–Taylor polarizer, rotated by $\approx 45°$ with respect to the polarization direction of the first, distributes the light onto two silicon avalanche photodetectors (APDs) that provide detection timing signals to a correlator. The relative orientation of the two polarizers allows for the balancing of the photodetection rates to optimize the integration time, and also helps to suppress the optical crosstalk between the two APDs due to hot carrier recombination in the devices upon detection which would otherwise introduce false coincidence events (Kurtsiefer et al. 2001).

The temporal correlation was carried out with a digital sampling oscilloscope (4 GHz analog bandwidth, 40 Gsamples/ sec, LeCroy) that recorded the APD signals if two detection events fall within a coarse coincidence time window of 20 ns. The oscilloscope then evaluated the timing difference τ between the APD events with an uncertainty below 10 ps, and generated a histogram of all observed τ. The temporal correlation function $g^{(2)}(\tau)$ is just a normalized version of this histogram.

To assess the overall timing uncertainty with the detector/ correlator combination, we exposed two different APD sets to photon pairs generated by spontaneous parametric down conversion (SPDC) with a coherence time below 10 ps. The resulting temporal correlations shown in Figure 3 reflect the overall timing resolution of the system. For APDs with a deep conversion zone (C30902S, Perkin–Elmer, passive quenching), the coincidence distribution appears roughly Gaussian, with 1.2 ns FWHM. Since the photon bunching signature $g^{(2)}(\tau)$
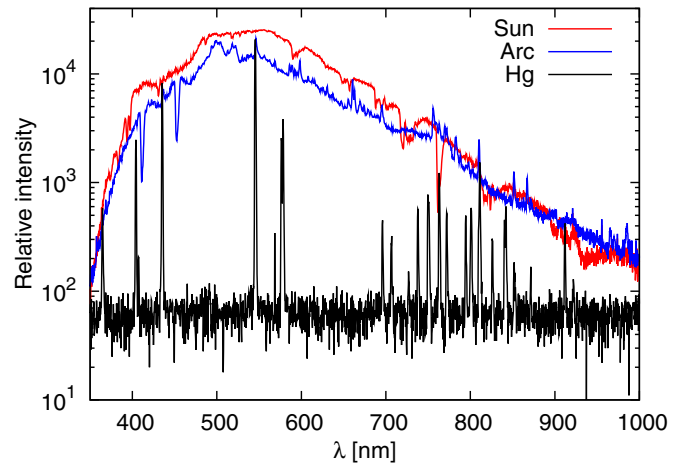

Figure 4. Spectrum of a Hg glow discharge lamp, an Ar arc lamp as a simulator of a stellar light source, and the Sun.

(A color version of this figure is available in the online journal.)

of the light field under investigation needs to be convolved with this detector response, we would observe a significant reduction of the photon bunching peak with these detectors. A second set of APDs, based on thin conversion zones (type PDF, Micro Photon Devices, active quenching), leads to a much better localized coincidence distribution with 40 ps FWHM, although a significant fraction of the distribution shows a tail with timing differences up to 500 ps.

4. RESULTS

Measurements for $g^{(2)}(\tau)$ using the high-bandwidth (type PDF) photon detectors were performed on three light sources: a low-pressure mercury (Hg) discharge lamp as a quasi-thermal light source, a radio frequency-driven argon (Ar) arc discharge lamp to produce a plasma with a blackbody temperature ≈ 6000 K as the thermal light source, and the Sun as a celestial thermal light source. Their respective spectral distributions are shown in Figure 4. The optical filters were fixed to maximize transmission for the spectral lines around 546.1 nm in the Hg spectrum. The resulting timing difference histograms are shown in Figure 5.

To ensure proper normalization of the resulting $g^{(2)}(\tau)$, we independently recorded pair events with a resolution of about 300 ps with a time stamp unit that, unlike the oscilloscope, does not exhibit a significant dead time varying with acquisition mode and event rate, and found that $g^{(2)}(|\tau| \gtrsim 2\,\text{ns}) \to 1$. To extract a meaningful set of model parameters, we assumed a Lorentzian line shape for the spectral power distribution; this is mostly to reflect the approximate etalon transmission function. A corresponding model function for the obtained pair rates in the histograms is

$$N(\tau) = a + b \cdot e^{-|2\tau/\tau_c|}, \qquad (3)$$

where a, b capture the absolute event number and the degree of bunching, respectively, while τ_c represents a coherence time. The $g^{(2)}$ scale on the right side of the diagrams in Figure 5 refers to the absolute number of events after division by fit parameter a.

For the Hg emission line at 546 nm from the low-pressure glow discharge lamp, coincidence data was obtained over an integration time of 68 hr, with single-detector rates of 115,000 s^{-1}. From the numerical fit, we find $g^{(2)}(\tau = 0) =$
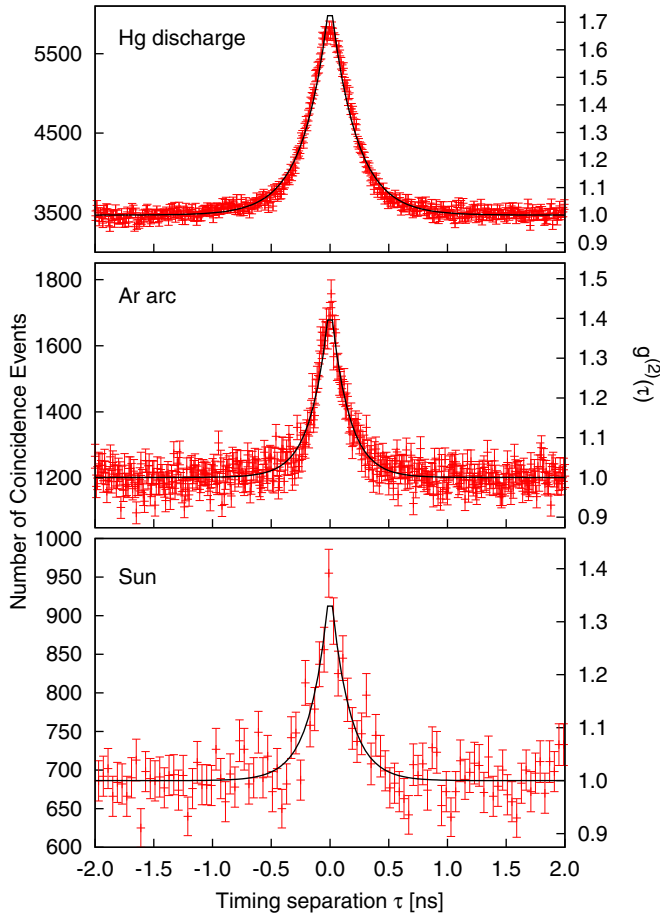
Figure 5. Intensity correlation function $g^{(2)}(\tau)$ from the three thermal light sources after spectral filtering. All light sources show a significant bunching at $\tau = 0$ and a decay time that is well resolved with the avalanche photodetectors. Error bars indicate uncertainties due to Poissonian counting statistics.

(A color version of this figure is available in the online journal.)

1.795 ± 0.006 and an exponential decay with a characteristic coherence time of $\tau_c = 0.436 \pm 0.006$ ns. A convolution of an ideal correlation function from a finite-bandwidth thermal light source (where $g^{(2)}(\tau = 0) = 2$) with the detector response recorded in Figure 3 leads to $g^{(2)}(\tau = 0) = 1.85$. Thus, the mercury lamp seems perfectly compatible with a thermal light source. The Doppler-broadened line width for individual transitions in Hg vapor at temperatures around 400 K is on the order of 235 MHz, but the contributions of different hyperfine transitions from different isotopes result in a complex overall line shape of several GHz width (see Figure 2(b)). The part of the spectrum we select with the etalon has a resultant coherence time that is slightly longer than what we would expect from a flat spectrum filtered by the etalon ($\tau_c \approx 0.34$ ns).

For the Ar arc discharge lamp, a wavelength of 540 nm was chosen to avoid contributions of a prominent peak at 546 nm, possibly caused by mercury traces in the plasma. We find that $g^{(2)}(0) = 1.45 \pm 0.01$ and a shorter coherence time $\tau_c = 0.31 \pm 0.01$ ns with $\chi_r^2 = 1.066$. The wider spectrum of the cutout blackbody radiation makes the decay time shorter, so a peak reduction due to the detector response becomes more prominent. Furthermore, residual transmission of the grating monochromator or stray light into other transmission peaks of the etalon may contribute to light that is incoherent with the main peak on observable timescales.

For an etalon of $R \approx 97\%$ and therefore an effective finesse of about 100, we expect a minimum transmission of $\approx 0.1\%$ over the whole grating transmission of ≈ 240 GHz (for two FWHMs). The etalon also has a less-than-ideal peak transmission of approximately 50%. The off-peak transmission of the etalon effectively serves as an additional incoherent light source that adds about 24% more photons than a single-peaked transmission with exponential decay. These additional random correlations further reduce the measured $g^{(2)}(\tau = 0)$ from 1.8 due to the detector resolution down to ≈ 1.5, which is in good agreement with the value of 1.45 measured for the Ar arc lamp.

We finally collected sunlight into a single-mode optical fiber with a coelostat and transferred it into the lab. At the same working wavelength of 546.1 nm, we find $g^{(2)}(0) = 1.37 \pm 0.03$ and a coherence time $\tau_c = 0.32 \pm 0.04$ ns, with $\chi_r^2 = 0.985$ over an integration time of 85 minutes, measuring the Sun near the zenith at an altitude of $77°$–$64°$. From an altitude of $32°$–$21°$ close to the horizon, we find $g^{(2)}(0) = 1.3 \pm 0.1$, $\tau_c = 0.26 \pm 0.05$ ns, with $\chi_r^2 = 1.024$ over 45 minutes. This apparent dependency of the measured visibility of the photon bunching on the altitude of the Sun is possibly due to seeing-induced atmospheric fluctuations in optical path length differences (Dravins 2007), where studies by Kral et al. (2004), Blazej et al. (2008), and Ortolani & Barbieri (2012) suggest that atmospheric turbulence and scintillation may introduce jitter in photon timing measurements and is strongly dependent on the altitude of the light source.

5. SUMMARY AND OUTLOOK

We have successfully developed and demonstrated an experimental technique to resolve the temporal structure of photon bunching from thermal blackbody light sources, including both discrete spectrum and blackbody spectra, such as the Sun. We observed a photon bunching signature, i.e., the excess of $g^{(2)}(0)$ above one, that exceeds the recently reported records of $g^{(2)}(0) = 1.03$ (Karmakar et al. 2012) and $g^{(2)}(0) = 1.04$ (Liu et al. 2014) by about an order of magnitude.

Compared to photon bunching observations using two-photon absorption (Boitier et al. 2009), our method would work at astronomical intensity levels and would, not be constrained to cases with the simultaneous arrivals of two photons at the same detector.

We believe that with better timing control of the photodetectors and a better match of the etalon with the grating monochromator as a first stage, it should be possible to reach the theoretical limit $g^{(2)}(0) = 2$ for blackbody radiators.

The ability to partially resolve temporal photon bunching information directly may allow for additional probing into the emission properties of light sources and extend the traditional scope of intensity interferometry of investigating the spatial coherence of a source. Even there, our filtering technique may help to address detector saturation and scintillation issues.

This filtering technique may also be used to measure the visibility of starlight at various redshifts, providing information on possible photon decoherence across extended distances unaccessible in Earth-based laboratory conditions. Such experiments may provide complementary observational evidence that help to set constraints in theoretical models of quantum gravity (Lieu & Hillman 2003; Ng et al. 2003; Ragazzoni et al. 2003; Maziashvili 2009).

REFERENCES

Asakura, T. 1970, Opto-electron., 2, 115
Blazej, J., Prochazka, I., & Kral, L. 2008, Proc. SPIE, 7152, 71520R
Boitier, F., Godard, A., Rosencher, E., & Fabre, C. 2009, NatPh, 5, 267
Castor, J. I., & Nussbaumer, H. 1972, MNRAS, 155, 293
Davis, J., Tango, W. J., Booth, A. J., et al. 1999, MNRAS, 303, 773
Dravins, D. 2007, High Time Resolution Astrophysics (Astrophysics and Space Science Library; Berlin: Springer)
Dravins, D., & Germanà, C. 2008, in AIP Conf. Proc. 984, The Universe at Sub-second Timescales, ed. D. Phelan, O. Ryan, & A. Shearer (Melville, NY: AIP), 216
Foellmi, C. 2009, A&A, 507, 1719 (eSO)
Fox, M. 2006, Quantum Optics: An Introduction (Oxford: Oxford Univ. Press)
Glauber, R. 1963, PhRv, 131, 2766
Green, J. M. 1980, JPhE, 13, 1302 (iOP)
Hanbury-Brown, R. 1974, The Intensity Interferometer: Its Application to Astronomy (London: Taylor & Francis), 184
Hanbury-Brown, R., Davis, J., & Allen, L. R. 1974, MNRAS, 167, 121
Hanbury-Brown, R., & Twiss, R. Q. 1954, PMag, 45, 663
Hanbury-Brown, R., & Twiss, R. Q. 1956, Natur, 178, 1046
Hanbury-Brown, R., & Twiss, R. Q. 1957, RSPSA, 242, 300
Karmakar, S., Meyers, R., & Shih, Y. 2012, Proc. SPIE, 8518, 851805
Kral, L., Prochazka, I., Blazej, J., & Hamal, K. 2004, Proc. SPIE, 5240, 26
Kurtsiefer, C., Zarda, P., Mayer, S., & Weinfurter, H. 2001, JMOp, 48, 2039
Lieu, R., & Hillman, L. W. 2003, ApJL, 585, L77
Liu, X.-F., Chen, X.-H., Yao, X.-R., et al. 2014, OptL, 39, 2314
Malvimat, V., Wucknitz, O., & Saha, P. 2013, MNRAS
Mandel, L., & Wolf, E. 1995, Optical Coherence and Quantum Optics (Cambridge: Cambridge Uni. Press)
Martienssen, W., & Spiller, E. 1964, AmJPh, 32, 919
Maziashvili, M. 2009, APh, 31, 344
Millour, F. 2008, NewAR, 52, 177
Morgan, B. L., & Mandel, L. 1966, PhRvL, 16, 1012
Ng, Y. J., Christiansen, W. A., & van Dam, H. 2003, ApJL, 591, L87
Nuñez, P. D. 2012, Masters thesis, Univ. Utah
Ortolani, S. C. S., & Barbieri, C. 2012, MNRAS, 419, 2349
Park, S., Ko, H., & Park, M.-H. 2005, OptEn, 44, 048001
Ragazzoni, R., Turatto, M., & Gaessler, W. 2003, ApJL, 587, L1
Rou, J., Nunez, P. D., Kieda, D., & LeBohec, S. 2012, MNRAS, 000, 1
Saleh, B. E. A., & Teich, M. C. 2007, Fundamentals of Photonics (2nd ed.; Hoboken, NJ: Wiley)
Sansonetti, C. J., & Veza, D. 2010, JPhB, 43, 205003
Scarl, D. B. 1968, PhRv, 175, 1661
van der Hucht, K. A. 2001, NewAR, 45, 135
Varshni, Y. P., & Nasser, R. M. 1986, Ap&SS, 125, 341

Q2
Q3
Q4
Q5
Q6
Q7
Q8

Queries

Page 1

Q1

Author: As per style, the acronym "SNR" used for the signal-to-noise ratio has been changed to "S/N" throughout the text. Please confirm if this is correct.

Page 5

Q2

Author: Please check the details for any journal references that do not have a pale purple link (CrossRef doi) or a blue link (NASA ADS or arXiv e-print) in the two-column proof (article-style layout). A journal reference with no links may contain some incorrect information.

Q3

Author: Please confirm whether in references "Blazej et al. (2008)," "Karmakar et al. (2012)," "Kral et al. (2004)," and "Martienssen & Spiller (1964)" the page numbers are correct as included.

Q4

Author: Please confirm whether in references "Dravins (2007)" and "Fox (2006)" the publisher locations are correct as included.

Q5

Author: Please confirm whether in reference "Dravins & Germanà (2008)" the conference series name, series number, publisher details (name and location), and page number are correct as included.

Q6

Author: Please provide the volume and page numbers in reference "Malvimat et al. (2013)."

Q7

Author: Please update the volume number in reference "Rou et al. (2012)."

Q8

Author: Please confirm whether in reference "Saleh & Teich (2007)" the edition number and publisher location are correct as included.

Online-only colour figures

This proof PDF is identical in specification to the PDF file that will be published in the online journal. To view any online-only color figures as they will appear in the printed journal, we recommend that this color PDF file be printed on a black & white printer.